Carbon and Insulation Materials Technology Group
Metals and Ceramics Division

CRADA Final Report
For CRADA C/ORNL-97-0483

The Development and Characterization of Novel Adsorbent Carbons

T. D. Burchell
Oak Ridge National Laboratory

and

F. S. Baker
Westvaco Corporation

Date Published February 2001

Prepared for Westvaco Corporation
Charleston, South Carolina

Prepared by the
OAK RIDGE NATIONAL LABORATORY
Oak Ridge, Tennessee 37831
Managed by
UT-BATTELLE, LLC
for the
U.S. DEPARTMENT OF ENERGY
Under contract DE-AC05-00OR22725

CRADA ORNL-97-0483 Final Report

THE DEVELOPMENT AND CHARACTERIZATION OF NOVEL ADSORBENT CARBONS

ABSTRACT

The Oak Ridge National Laboratory (ORNL) and the Westvaco Corporation are both engaged in the development of novel adsorbent carbons. This CRADA facilitated close cooperation between these partners in the characterization and performance of several novel adsorbent carbon materials. The research and development activities conducted under this CRADA fell into three major areas:

(1) The determination of the methane storage capacities of ORNL's adsorbent carbon monoliths.
(2) The determination of the thermal conductivity of ORNL's adsorbent carbon monoliths and Westvaco's powdered activated carbon product.
(3) The use of X-ray diffraction analysis to characterize the structure of Westvaco's powdered activated carbon and investigate structural changes after heat-treatment to high temperatures.

The results of activities in these three areas are reported and discussed here.

1. OBJECTIVES AND BACKGROUND

The purpose of this Cooperative Research and Development Agreement (CRADA) between the Oak Ridge National Laboratory (ORNL) and Westvaco Corporation was the development and characterization of adsorbent carbons, with an emphasis on carbon fiber based monoliths of the type already developed at ORNL.

Specialty activated carbons are widely used in gas separation, purification, and storage applications. For example, odor removal, solvent recovery, emission traps, and gas masks. Typically, the activated carbon is in the form of powder, granules, or extruded pellets. A novel, monolithic, specialty activated carbon has been developed by ORNL that is based on isotropic pitch-derived carbon fibers. The fiber-based monolithic adsorbent carbon has several potential advantages over granular and pelletized activated carbons. During service, monoliths are not prone to attrition and dust formation, unlike granular carbons that are subject to attrition under conditions of severe service. The formation of carbon dust can reduce the efficiency of separation equipment by increasing pressure drop. Moreover, granular carbon beds may settle during operation, resulting in channels that allow by-pass flows, also reducing efficiency. Monoliths would be expected to be immune to these problems. Because of the small diameter (10-20 μm) of

the carbon fibers used in ORNL's monoliths, they offer a kinetic advantage over granules and extrudates, which typically have dimensions (diameters and lengths) of several mm.

The density and micro/meso pore size can be controlled in the fiber-based monoliths by variation of the fiber precursor, processing route, and activation method. Therefore, the monoliths can be tailored to specific gas storage and separation applications. Moreover, the monoliths posses a continuous carbon skeleton and thus are electrically conductive. When an electric current flows through the material at low voltage the carbon monoliths may be readily heated to temperatures > 100°C. This offers the potential of a simple, low-energy route to desorb gasses and regenerate the monoliths in gas storage, purification, and separation applications.

The objectives of this CRADA therefore were to explore the gas storage/separation behavior of the monoliths, and to study the structure and properties of novel adsorbent carbons from Westvaco Corporation and ORNL.

2. RESULTS AND DISCUSSION

2.1 Determination of Methane Storage Capacity

The low-pressure storage of natural gas in the physically adsorbed state is of interest to the DOE. Westvaco has developed adsorbent carbons for gas storage, test equipment and a test methodology for the determination of the methane storage capacity of carbons. Several samples of an adsorbent carbon, based on isotropic pitch-derived carbon fibers, were supplied to Westvaco for methane capacity determination. The adsorbent carbons were developed as part of a program funded by the DOE's Office of Heavy Vehicle Technologies. The manufacturing process is illustrated in Fig. 1.

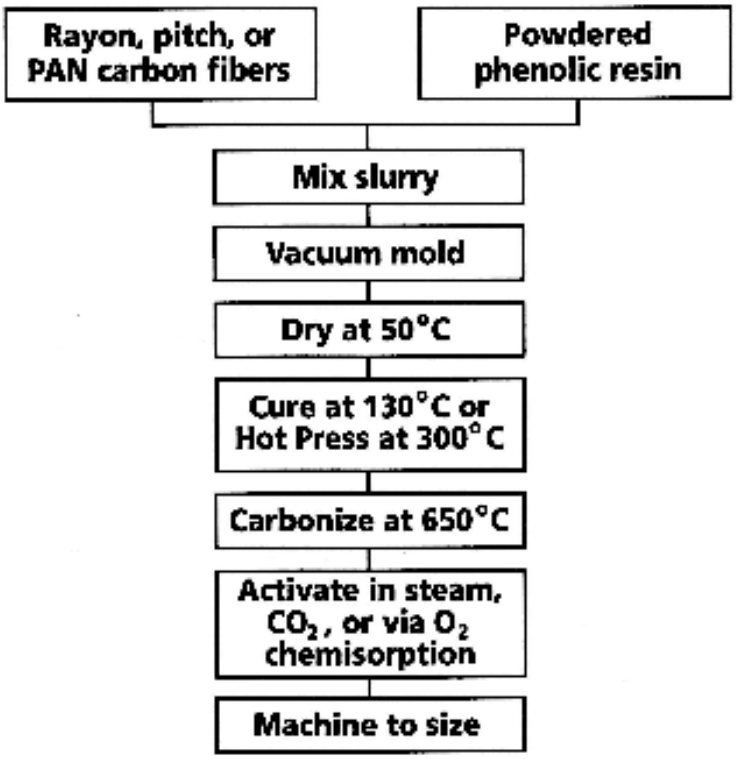

Figure 1. The manufacturing process for ORNL's gas storage monoliths.

The monoliths were sampled after activation and subjected to micropore analysis at ORNL, requiring the measurement of a nitrogen adsorption isotherm at a temperature of 77K, from which the micropore size distribution, micropore volume, and BET surface area were calculated. Typical N_2 adsorption isotherms for two of ORNL's monoliths are in Figs. 2 and 3. The N_2 adsorption isotherms are type 1, which is characteristic of microporous materials (pore size < 2 nm). The DA micropore size distributions shown in Figs. 4 and 5 for the same materials, confirm their microporous nature.

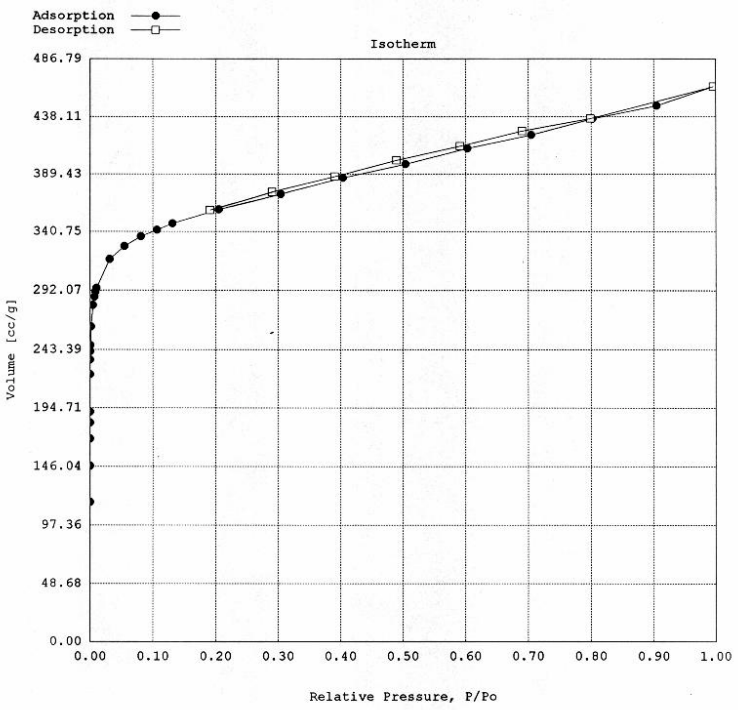

Figure 2. Nitrogen adsorption isotherm for natural gas adsorption monolith SMS-3B

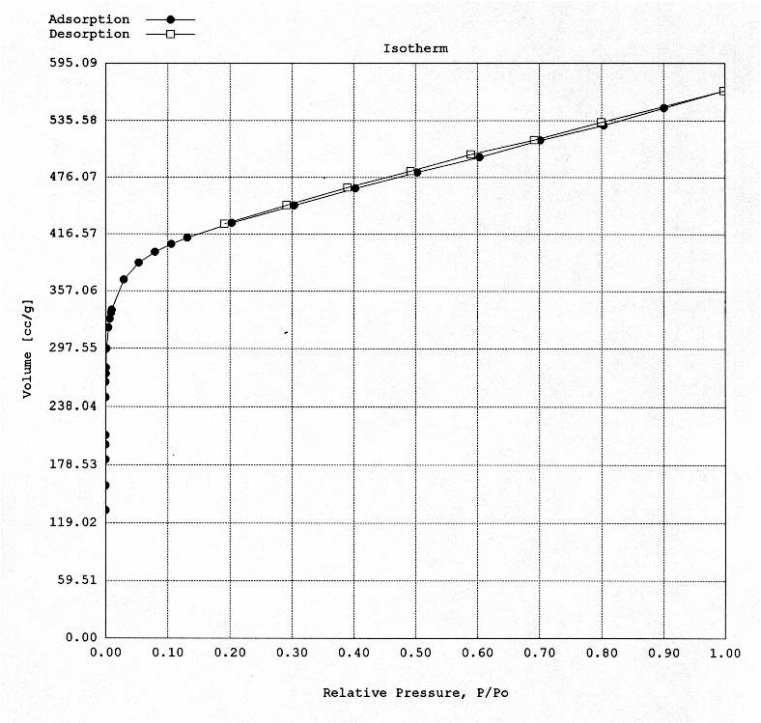

Figure 3. Nitrogen adsorption isotherm for natural gas adsorption monolith SMS-5A

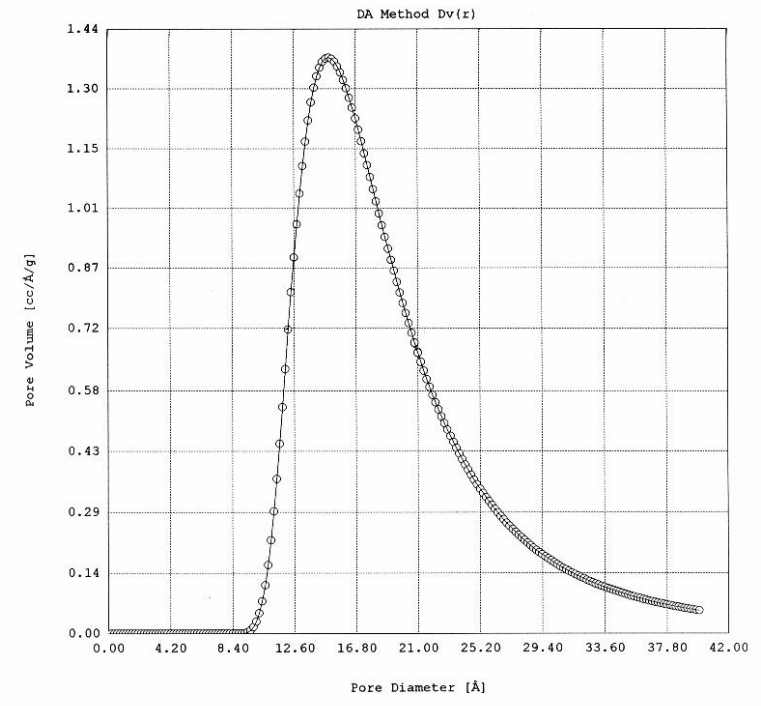

Figure 4. DA micropore size distribution for natural gas adsorption monolith SMS-3B

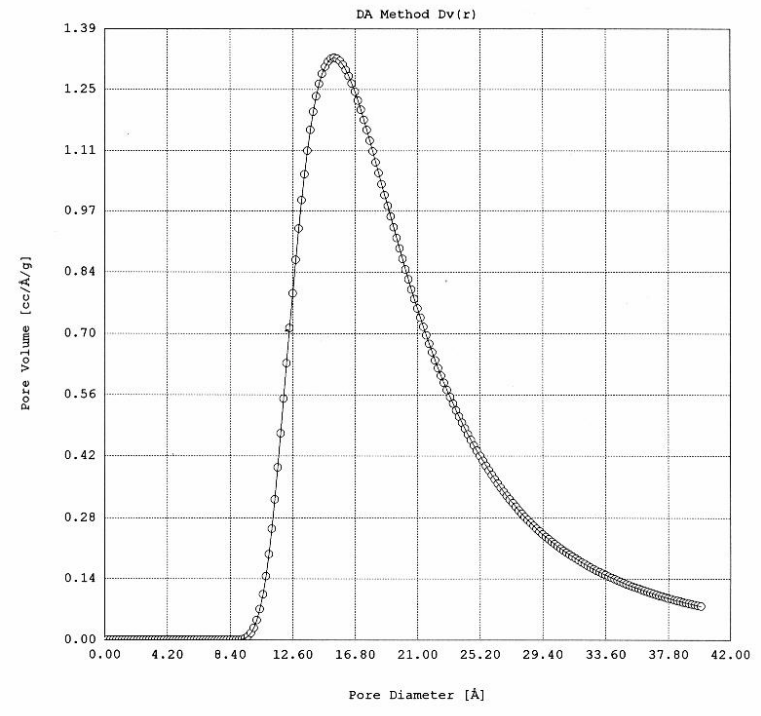

Figure 5. DA micropore size distribution for natural gas adsorption monolith SMS-5A

The micropore characterization data obtained for monolith SMS-3B and -5A are summarized in Table 1 below.

Table 1. Micropore characterization data obtained for monolith SMS-3B and -5A

Nitrogen Adsorption Analysis Data			
Sample Number	**BET Surface Area (m^2/g)**	**DR Micropore Volume (cm^3/g)**	**DR Micropore Size (nm)**
SMS-2B	961	0.36	1.60
SMS-3B	1283	0.49	1.90
SMS-5A	1608	0.60	2.00
SMS-6	1907	0.70	2.10
SMS-7	1819	0.67	2.10
SMS-8	2112	0.76	2.20
SMS-9	2334	0.83	2.30
SMS-10	2670	0.92	2.50

The methane storage capacity of the above monoliths was determined gravimetrically and the following five important parameters were calculated from the experimental data:

- Cell pack density (g/cm^3)
- Methane weight activity of carbon, M_A (wt%)
- Total methane storage capacity, M_T (V/V)
- Deliverable methane capacity, M_D (V/V)
- Methane retentivity of the carbon, M_R (wt%)

The equations used to calculate the adsorption data are reported below.

Cell pack density (g/cm^3)

Cell pack density = M_c/V_c

where M_c is the outgassed (dry) mass of carbon in the cell (grams) and V_c is the cell volume in cubic centimeters.

The methane weight activity of the carbon, M_A (wt %)

This value is calculated by expressing the mass of gas adsorbed on the carbon as a percentage of the dry mass carbon sample. The mass of gas adsorbed on the carbon is obtained by correcting the total mass of gas in the test cell by subtracting the mass of gas in the void space at the test pressure.

$$M_A = \left\{ \frac{M_a - \left[\left(V_v - \frac{M_c}{2} \right) \times \left(\frac{16.04}{22414} \right) \times \left(\frac{273}{273 + T_a} \right) \times \left(\frac{P_a + 14.7}{14.7} \right) \right]}{M_c} \right\} \times 100$$

where:

M_A = mass of gas **adsorbed** (wt%) at pressure P_a (psig) and temperature T_a (°C).
M_a = total mass of gas in the test cell (g) at pressure P_a, usually 500 psig.
M_c = mass of "dry" carbon sample, i.e., after outgassing (g).
P_a = pressure of measurement (psi), usually 500 psig.
T_a = ambient temperature of measurement (°C), usually 25°C.
V_v = volume of empty test cylinder (cm^3).
2 = assumed structural density of activated carbon (g/cm^3).
22,414 = molar volume of methane at STP.
16.04 = molecular weight of methane.
273 = standard temperature (K).
14.7 = standard pressure (psia).

NB. The STP density of methane is (16.04/22414) = 7.16×10^{-4} g/cm^3.

Total methane storage capacity, M_T (V/V)

This value is expressed at 25°C by convention.

$$M_T = \frac{M_a \times \left(\frac{22414}{16.04} \right) \times \left(\frac{298}{273} \right)}{V_v}$$

where

M_a = total mass of gas in the test cell (g) at pressure P_a, usually 500 psig.
V_v = volume of empty test cylinder (cm^3).
22,414 = molar volume of methane at STP.
16.04 = molecular weight of methane.

Deliverable methane capacity, M_D (V/V)

This is the amount (storage capacity) of methane deliverable when the cell is discharged to atmospheric pressure (at 25°C):

$$M_D = \frac{(M_a - M_r) \times \left(\frac{22414}{16.04}\right) \times \left(\frac{298}{273}\right)}{V_v}$$

where

M_a = total mass of gas in the test cell (g) at pressure P_a, usually 500 psig.
M_r= mass of gas retained in the cell at atmospheric pressure and room temperature.
V_v = volume of empty test cylinder (cm^3).
22,414 = molar volume of methane at STP.
16.04 = molecular weight of methane.

Methane retentivity of the carbon, M_R (wt%)

This is the percentage of methane retained on the carbon after draw down to atmospheric pressure. A low retentivity is desirable.

$$M_R = \left\{ \frac{M_r - \left[\left(V_v - \frac{M_c}{2} \right) \times \left(\frac{16.04}{22414} \right) \times \left(\frac{273}{273 + T_a} \right) \times \left(\frac{P_a + 14.7}{14.7} \right) \right]}{\frac{M_A \times M_c}{100}} \right\} \times 100$$

where

M_r = mass of gas retained in the test cell (g) at atmospheric pressure (i.e., zero psig).
M_a = total mass of gas in the test cell (g) at pressure P_a, usually 500 psig.
M_A = mass of gas **adsorbed** (wt%) at pressure P_a (psig) and temperature T_a (°C).
M_c = mass of "dry" carbon sample, i.e., after outgassing (g).
P_a = pressure of measurement (psi), usually 500 psig.
T_a = ambient temperature of measurement (°C), usually 25°C.
V_v = volume of empty test cylinder (cm^3).
2 = assumed structural density of activated carbon (g/cm^3).
22,414 = molar volume of methane at STP.
16.04 = molecular weight of methane.
273 = standard temperature (K).
14.7 = standard pressure (psia).

The methane adsorption data is summarized in Table 2 below for the monoliths tested at Westvaco.

Table 2. Methane storage data for the ORNL monoliths tested at Westvaco

Methane Storage Data					
Sample Number	**Cell Pack Density (g/cc)**	**Methane Weight Activity of Carbon (wt %)**	**Total Storage Capacity @298K (V/V)**	**Deliverable Methane Capacity @298K (V/V)**	**Methane Retentivity of Carbon (wt %)**
SMS-2B	0.47	6.8	76	61	29.0
SMS-3B	0.42	8.9	84	71	23.0
SMS-5A	0.53	9.8	104	87	20.0
SMS-6	0.47	10.6	102	87	18.0
SMS-7	0.42	11.6	103	89	18.0
SMS-8	0.45	10.8	100	85	21.0
SMS-9	0.48	11.6	111	91	22.0
SMS-10	0.46	12.0	110	91	22.0

The methane capacity data indicates the importance of attaining a large weight activity of methane (a function of the micropore volume and micropore size) and a high pack density (a function of the monolith pre-activation density and the degree of activation or burn-off). A comparison of the data for SMS-5A and SMS-10 illustrates this point. The pack density of SMS-5A was 0.53 g/cm^3 and the methane activity only 9.8%, yet the monolith stored 104 V/V of methane. Conversely, SMS-10 had a higher methane activity (12%) and a lower pack density (0.46 g/cm^3), but stored 110 V/V of methane.

2.2 Thermal Conductivity of Adsorbent Carbons

2.2.1 ORNL monoliths

A series of ORNL monoliths with increasing amounts of high thermal conductivity mesophase pitch-derived carbon fibers were prepared for thermal conductivity determination. The thermal conductivity was measured using the thermal flash technique (ASTM C-714 and C-781). The thermal conductivity was calculated from the measured thermal diffusivity using the equation:

$$\text{Thermal conductivity, } \lambda = \alpha \bullet C_p \bullet \rho \quad (\text{W/m.K})$$

where α is the thermal diffusivity (m^2/s), C_p is the specific heat at the measurement temperature (J/kg.K), and ρ is the bulk density (kg/m^3). Table 3 reports the fractions of mesophase derived pitch fiber in each monolith and the bulk density of the monolith.

Table 3. Mesophase fiber content and bulk density for hybrid monoliths

Sample Identity	Fraction of Mesophase Fibers, %	Bulk Density, g/cm^3
K0A	0	0.606
K1A	5	0.644
K2A	11	0.645
K3A	18	0.634

The calculated thermal conductivity of samples K0A, K1A, K2A, and K3A are reported in Table 4 below for the temperature range 25–500°C. The thermal diffusivity was measured in the direction parallel to the fibers (i.e., perpendicular to the molding direction).

Table 4. Thermal conductivity data for ORNL's hybrid monolith

Temperature, °C	Thermal Conductivity, W/m.K			
	K0A	K1A	K2A	K3A
25	0.25	0.33	0.49	0.93
50	0.28	0.36	0.53	1.01
100	0.32	0.41	0.59	1.12
150	0.35	0.45	0.64	1.21
200	0.38	0.49	0.69	1.29
250	0.40	0.51	0.73	1.34
300	0.43	0.54	0.76	1.41
350	0.44	0.56	0.80	1.46
400	0.46	0.58	0.81	1.47
450	0.47	0.59	0.83	1.49
500	0.49	0.61	0.85	1.52

The thermal conductivity of each sample is plotted in Fig. 6 below. For all samples the thermal conductivity increased with temperature and with increasing fraction of mesophase pitch-derived fibers. The thermal conductivity of the monolith K0A (100% isotropic pitch-fiber) is approximately 3 times greater than for a packed bed of adsorbent powder (see Section 2.2.2 below). This difference would be expected to reduce in the case of activated monoliths because of the reduced density and increased structural disorder.

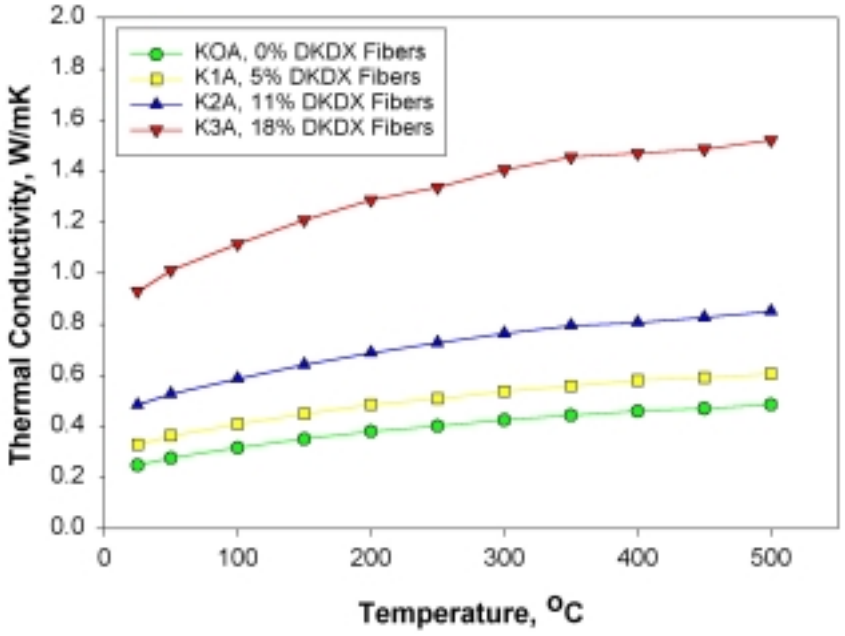

Figure 6. The temperature dependence of thermal conductivity for ORNL's hybrid monoliths

2.2.2 Westvaco activated carbon

Thermal conductivity measurements were made on a Westvaco activated carbon product using the ASTM C-518 method. Powdered carbon, 50 x 200 mesh, was poured into a frame that comprised polystyrene foam walls about half-an-inch thick, with a thin Tyvek[J] sheet at the bottom. The internal dimensions of the frame, i.e., of the carbon bed, were 10.8" square by 2" deep (about 27 x 27 x 5 cm). Using a vibratory technique, beds of carbon were packed to densities of 0.31, 0.37, and 0.42 ml/g, respectively. The frame containing the carbon bed was sandwiched between two plates, with the top plate in direct contact with the carbon, and placed in the heat flow equipment. The carbon bed

was held at the target temperature in the range of 5 to 50°C. A temperature differential of 22.2°C was applied between the plates, and the heat flux through the carbon was measured over the central 4" by 4" (10 x 10 cm) area of the bed using heat flux transducers in the top and bottom plates. The thermal conductivity (λ) of the carbon bed at a given temperature was measured as the temperature of the bed was increased step-wise to the upper target level of 50°C. The temperature of the bed was then lowered to 25°C, and a second measurement made at this temperature to check the reproducibility of the procedure.

The thermal conductivity data obtained are shown in Table 5 and Fig. 7. The thermal conductivity of the carbon bed increased as functions of temperature and packing density (for carbon beds of constant dimensions). The thermal conductivity of the carbon is summarized in Table 6 for the three bed densities at 20 and 40°C.

Table 5. The thermal conductivity of Westvaco activated carbon product

Temperature (°C)	Thermal Conductivity, λ (W/m.K)					
	Packing Density = 0.31 g/ml		Packing Density = 0.37 g/ml		Packing Density = 0.42 g/ml	
	Heating	Cooling	Heating	Cooling	Heating	Cooling
5	0.0676		0.0747		0.0807	
10	0.0687		0.0759		0.0818	
15	0.0700		0.0771		0.0828	
20	0.0714		0.0784		0.0539	
25	0.0733	0.0718	0.0198	0.0791	0.0851	0.0846
30	0.0762		0.0815		0.0864	
40	0.0817		0.0836		0.0881	
50	0.0912		0.0882		0.0906	

Table 6. Influence of bed packing density on thermal conductivity of Westvaco carbon

Packing Density (50 X 200 mesh, ml/g)	Thermal Conductivity, λ (W/m.K)	
	20°C	40°C
0.31	0.0714	0.0817
0.37	0.0784	0.0882
0.42	0.0839	0.0906

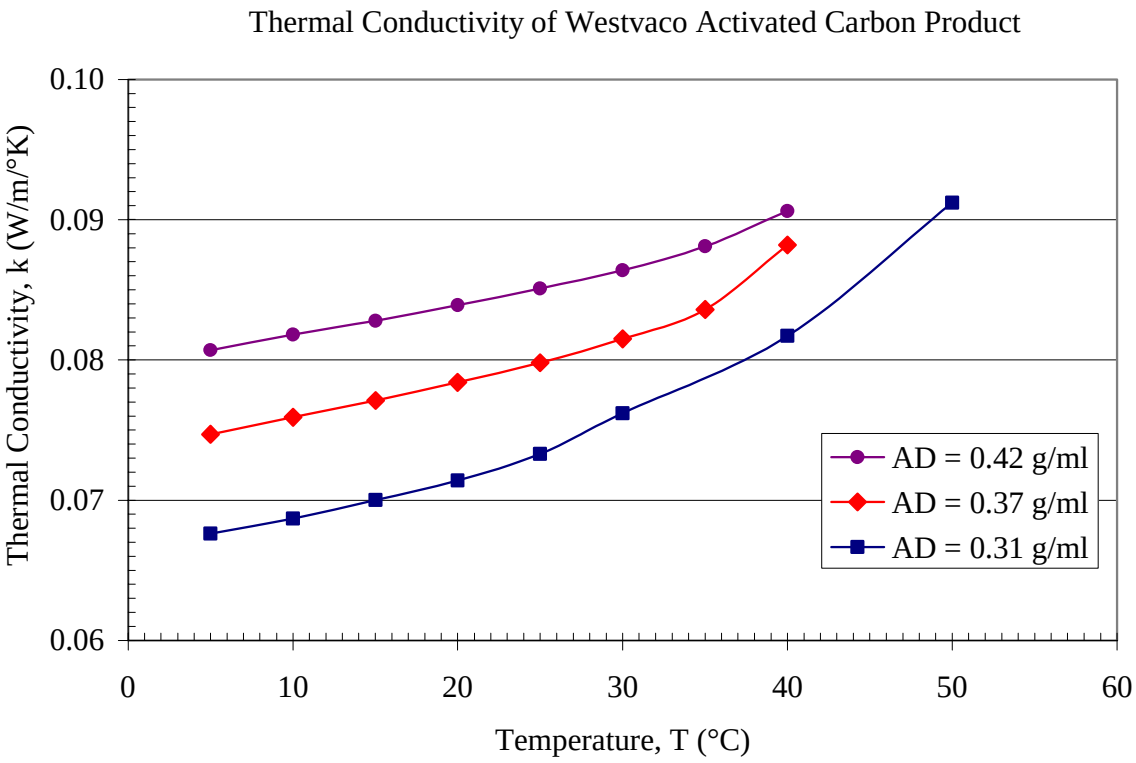

Figure 7. The temperature dependence of the thermal conductivity of Westvaco activated carbon product

The observed increase in thermal conductivity with increasing measurement temperature, for both of the carbons discussed above, can be attributed to the increasing contribution of in-pore radiation to the overall thermal conductivity. Radiation conductivity scales with the temperature to the third power and thus would be expected to influence the total thermal conductivity of both packed beds of Wesvaco Corporation's powdered carbon and ORNL's fiber based monoliths.

2.1 The Effects of Heat Treatment on the Structure of Activated Carbon

Samples of two Westvaco adsorbent carbons, designated A and B here, were heat treated to determine the effects of exposure to high temperatures on structure development. Table 7 below summarizes the heat treatments performed at ORNL.

Table 7. Summary of heat treatment conditions

Temperature (°C)	Time (hours)	Atmosphere	Samples
2000	2	Argon	B only
3000	2	Argon	A and B
3000	7.5	Argon	B only

X-ray diffaction (XRD) studies were performed on several samples from above along with a sample of Carbon-A in the as-received condition and an artificial graphite. The materials studied, their condition, and the corresponding XRD run number are shown in Table 8 below.

Table 8. XRD sample history

Sample	History	XRD Run Number
Artificial Graphite	As-received	1326
Westvaco-A	As-received	1330
Westvaco-A	3000°C for 2 hrs	1359
Westvaco-B	3000°C for 7.5 hrs	1360

The XRD analayses were performed using Cukα radiation with a wavelength, λ, of 1.540562Ο over an angular range of 10 to 90°. The crystal structure of graphite is shown in Fig. 8.

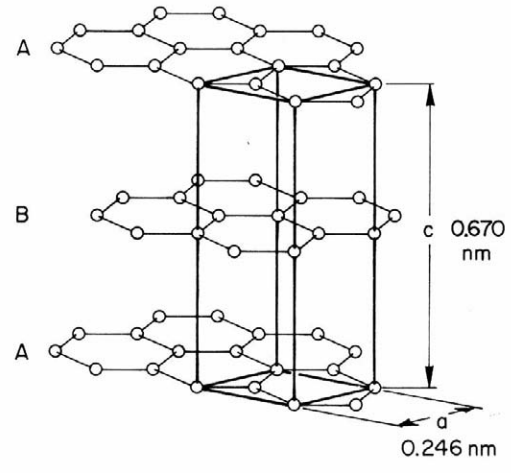

Figure 8. The crystal structure of graphite

Graphite consists of planar arrays of carbon atoms bound in a hexagonal lattice and stacked in an ABAB... sequence. In a perfect graphite crystal the spacing between adjacent aligned planes, or <c> spacing, is 0.6708 nm, and the spacing between prismatic edge carbon atoms, or <a> spacing, is 0.2461 nm (Fig. 8). These crystalographic features give rise to X-ray diffraction according to the Bragg Law which relates the wavelength of the incedent X-ray beam (λ) to the interplanar spacing (d) though the Bragg equation:

$$n\lambda = 2d \sin\theta$$

where n is an interger equal to the order of reflection and θ is the angle that the incident and reflected beams form with the plane. The <c> and <a> planes give rise to strong diffraction peaks at $2\theta = 26.603°$ (002) and $2\theta = 77.697°$ (110). The relevent parts of the diffraction pattern for the artificial graphite examined here are shown in Figs. 9 and 10. A comparison of Figs. 9 and 10 shows that the (002) peak is several orders of magnitude stronger than the (110) peak.

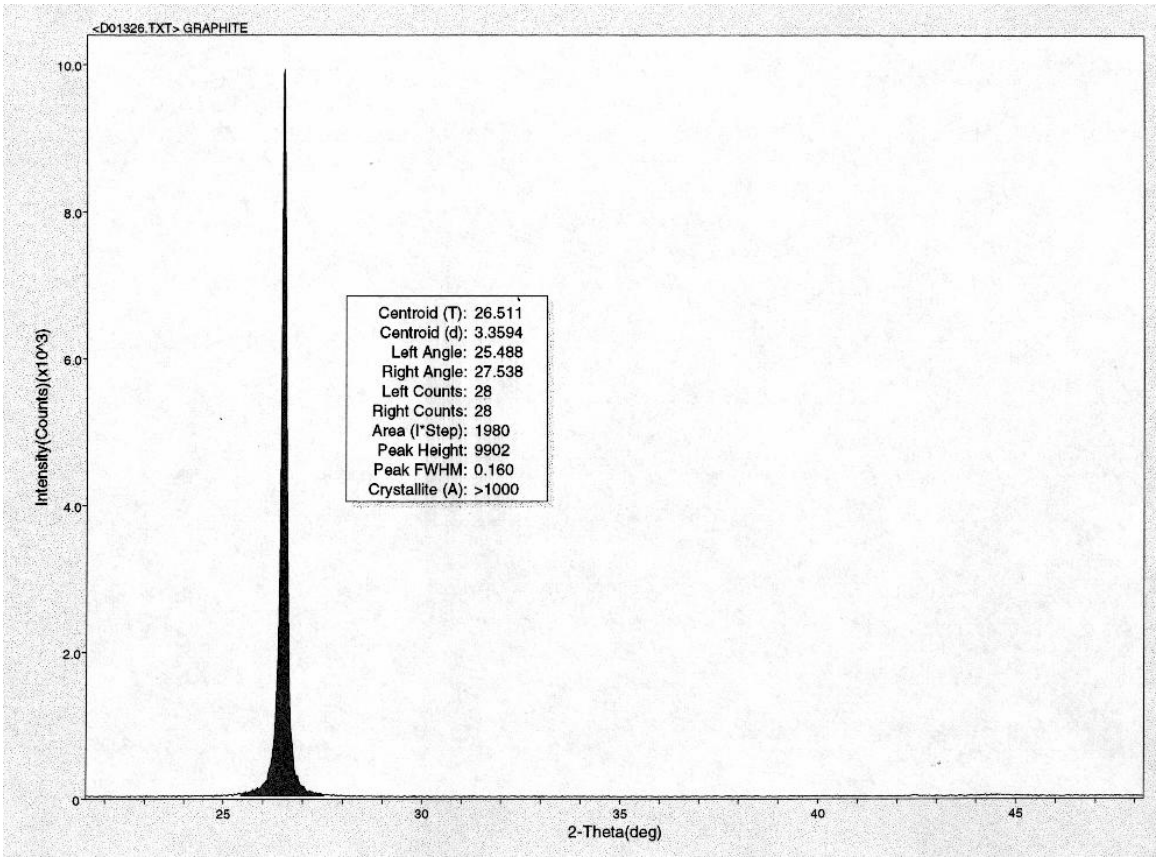

Figure 9. X-ray diffraction pattern from $2\theta = 21°$ too $2\theta = 48°$ showing the (002) peak for artificial graphite

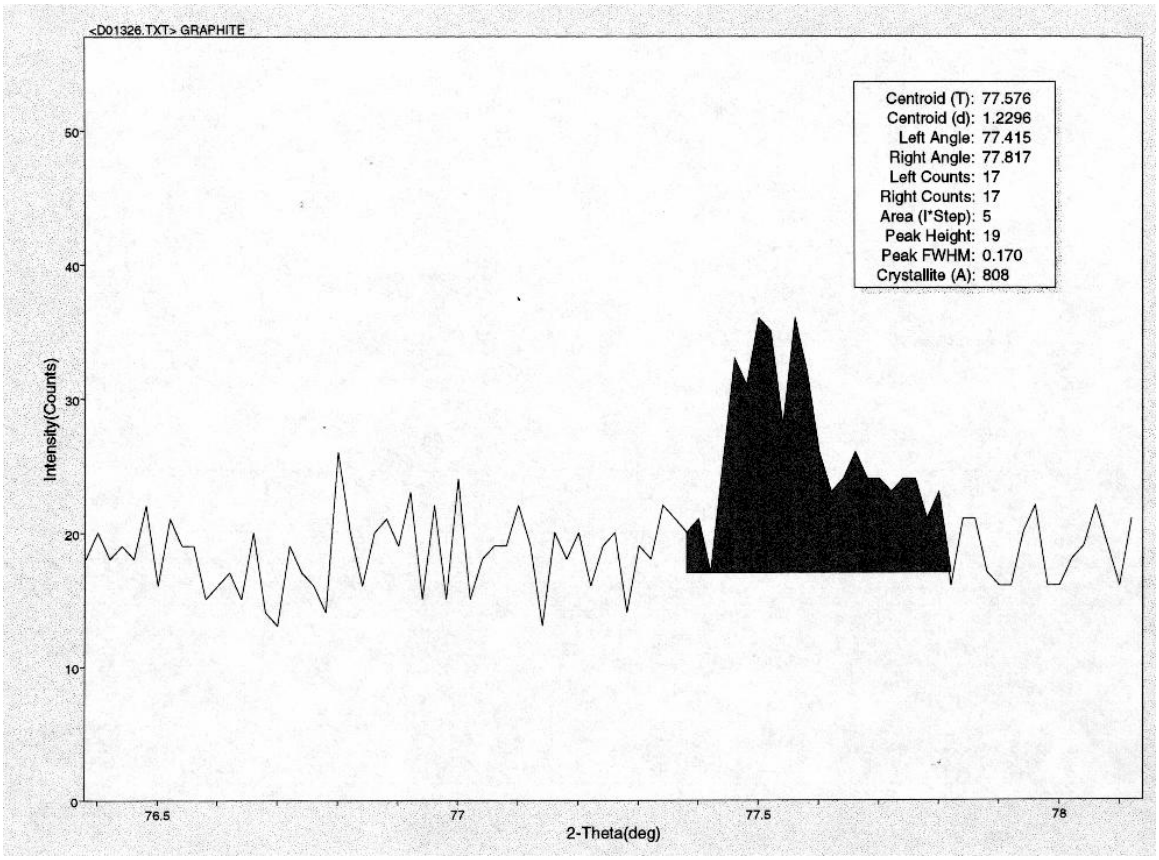

Figure 10. X-ray diffraction pattern from 2θ = 76.4° to 2θ = 78.1° showing the (110) peak for artificial graphite

Two further cyrstallographic parameters that are derived from the XRD data are the apparent crystallite size, or region of coherence, in the <a> and <c> directions. These parameters, denoted L_a and L_c for the <a> and <c> directions, respectively, are calculated from the Scherrer equation:

$$L = K\lambda / \beta \cos\theta$$

Where K is a shape factor equal to 1 for highly graphitic materials and equal to 1.84 for poorly ordered carbons, β is the intrinsic breadth of the diffraction peak (the full width at half maximum or FWHM value of the relevent difraction peak), and θ is the diffraction angle of the relevent peak. Note that the measured peak width must be corrected to allow for machine line broadening effects. In this work the machine correction factor was 0.06° (i.e., β = FWHM - 0.06°). The mean crystallite thickness, Lc, measured in the <c> direction is usually calculated from the (002) peak, whereas the mean crystallite length, La, measured in the <a> direction is normally measured from the (110) peak.

Figures 11–13 show the XRD patterns for the three Westvaco powdered carbons reported in Table 8.

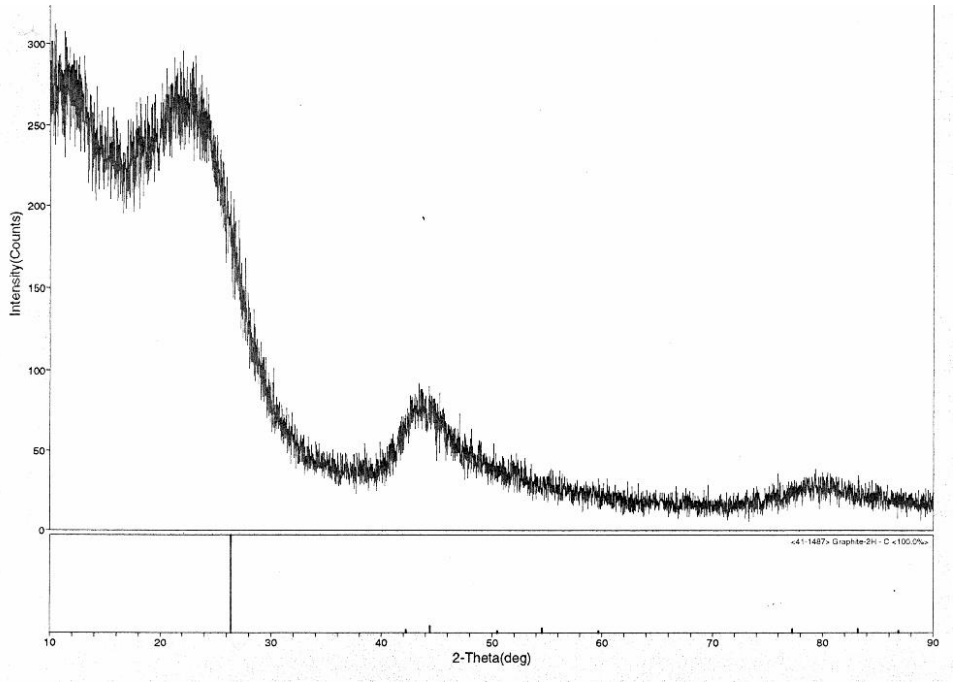

Figure 11. X-ray diffraction pattern from 2θ = 10° to 2θ = 90° showing the (002) and (110) peaks for Westavaco carbon-A in the as-received condition

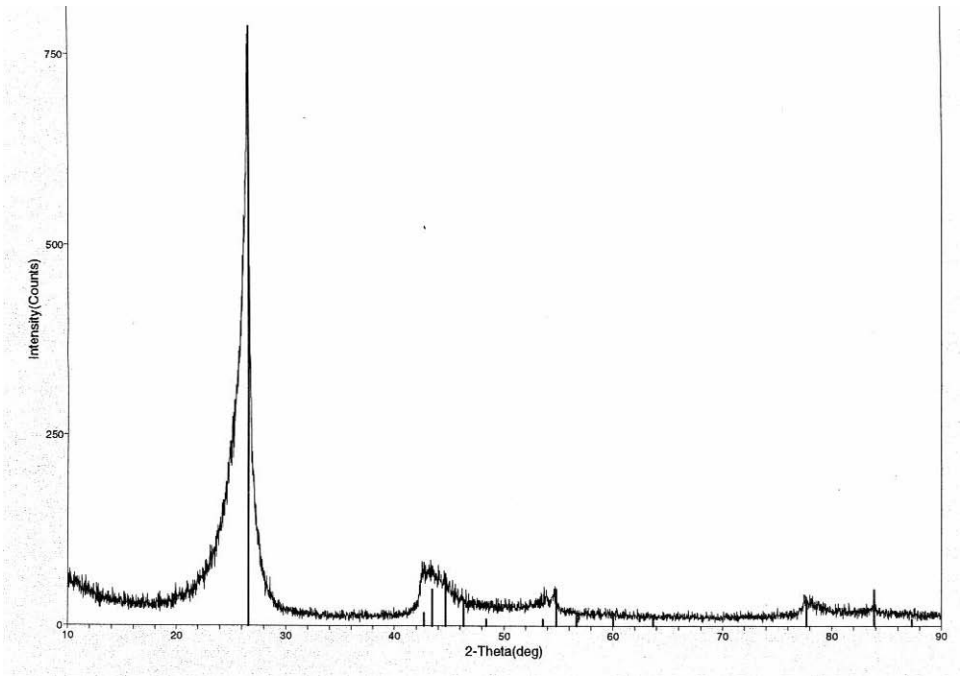

Figure 12. X-ray diffraction pattern from 2θ = 10° to 2θ = 90° showing the (002) and (110) peaks for Westavaco carbon-A after heat treatment at 3000°C for 2 hours

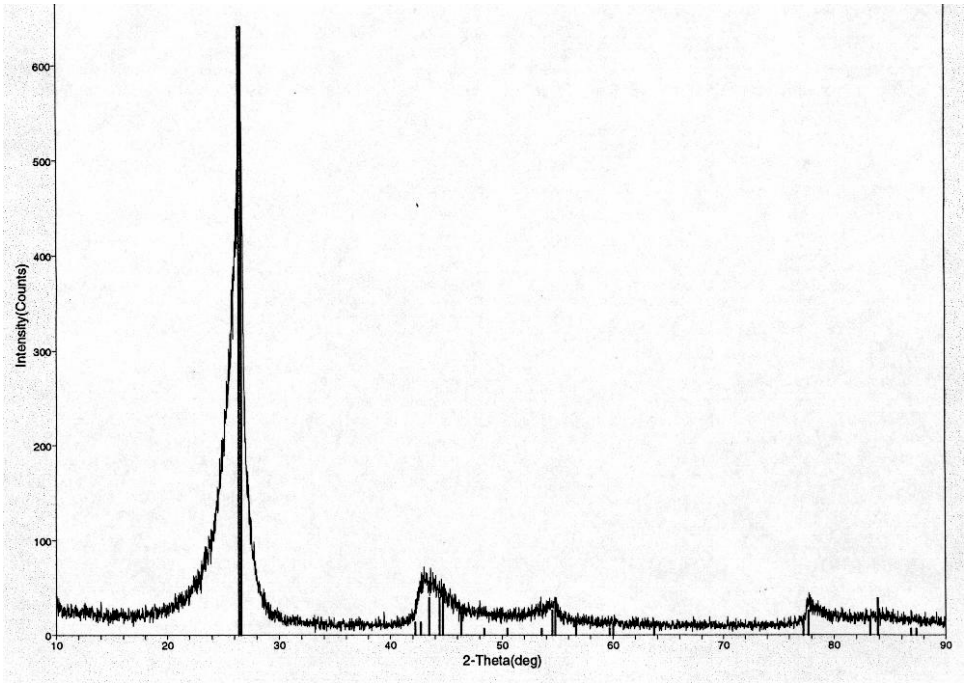

Figure 13. X-ray diffraction pattern from 2θ = 10° to 2θ = 90° showing the (002) and (110) peaks for Westavaco carbon-B after heat treatment to 3000°C for 7.5 hours

Inspection of Fig. 11 shows the Westvaco Carbon-A (as-received) to be a disordered carbon. The major peaks - (002) at ~ 26.5°, (101) at ~ 44.6°, and (110) at ~ 77.6° are all broad, poorly defined, and shifted from their normal positions (indicating different interplanar spacings compared to perfect graphite). The effects of heat treatment on the Westvaco carbons is readily discerned from Figs. 12 and 13. The (002) peak at ~ 26.5° is considerably sharper and more well-defined than the "as-received" sample, as are the (110) and (101) peaks. The number of counts associated with the (002) peak is increased in the heat treated samples by about a factor of two. However, the number of counts associated with the (002) peak in the heat treated samples (Figs. 12 and 13), ~ 700, is very small compared with that for the (002) graphite peak, ~ 10,000 (see Fig. 10).

The calculated crystal parameters for the carbon examined here are reported in Table 9. The values from the artificial graphite sample are typical of those reported in the literature for manufactured graphite [1]. Moreover, the parameters for the "as-received" Westvaco carbon-A are typical of those of a carbon black [1]. Heat treatment of Westvaco carbon-A has improved the crystalinity as indicated by the reduction in <c> spacing, and the increases in L_a and L_c.

Table 9. Crystal parameters for the four carbon materials examined here as calculated from the XRD patterns

Sample	Condition	Crystal Parameters			
		L_a (Å)	L_c (Å)	<a> (Å)	<c> (Å)
Artificial Graphite	As-recieved	534.11	1277.2	2.4596	6.7190
Westvaco A	As-received	15.358	15.001	2.3979	7.8709
Westvaco A	3000°C for 2 hrs	65.227	37.793	2.4479	6.6926
Westvaco B	3000°C for 7.5 hrs	333.42	31.938	2.4552	6.6906

3. BENEFITS TO THE DOE OFFICE OF FOSSIL ENERGY'S MISSION

Adsorbent carbons are increasingly being used in fossil fuel gas processing and separations. Moreover they have great potential for the low pressure storage of Natural Gas. Therefore, the development of new and improved adsorbent carbons would benefit ongoing DOE Fossil Enrgy programs in the areas of natural gas, clean coal technologies, and CO_2 capture.

4. INVENTIONS

None.

5. COMMERCIALIZATION POSSIBILITIES

None at present

6. PLANS FOR FUTURE COLLABORTAION

None at present.

7. CONCLUSIONS

The work conducted under this CRADA benefited both Westvaco Corporation and ORNL. Experimental data was obtained that would otherwise have been unavailable to the parties. The experimental work performed fell into three distict areas: (1) methane gas storage, (2) activated carbon thermal conductivity, and (3) the effects of heat treatment on carbon structure development.

The potential of ORNL's isotropic pitch-based carbon fiber monoliths to store methane gas via physical adsorption was succesfully demonstrated through a series of gas storage capacity measurements made by Westvaco. A total storage capacity of >100 V/V was

obtained. The work highlighted the need for both a large weight activity of methane and a high monolith pack density in order to realize improved storage capacities.

Thermal conductivity measurements made by ORNL on samples of Westvaco powdered activated carbon revealed a strong dependancy of the thermal conductivity on the bed packed density. Adsorbent monoliths prepared by ORNL exhibited a dependency of their thermal conductivity on the fraction of mesophase derived carbon fibers in the monolith. Both types of adsorbent carbon examined here exhibited an increasing thermal conductivity with temperature. This was attributed to an increased contribution to the overall themal conductivity from in-pore/void radiation, which varies with temperature to the third power.

Several samples of Westvaco powderd activated carbon were characterized using XRD. The diffraction patterns obtained were typical of disordered carbons. Several samples were heat treated to elevated temperature and subjected to XRD analysis to determine what sturctural changes may have occurred. Defined peaks at $2\theta = 26.5°$, 44.6°, and 77.6° suggest that heat traetment to 3000°C had induced substantially improved structural order to the carbon.

8. REFERENCES

1. R. E. Nightingale. *Nuclear Graphite*, Pub. Academic Press, New York, 1962.

9. ACKNOWLEDGEMENTS

This work was supported through a CRADA with Westvaco Corporation, Charleston, South Carolina, sponsored by the Office of Fossil Energy, Advanced Research Materials Program, (DOE/FE AA 15 10 10 0) U.S. Department of Energy under Contract DE-AC05-00OR22725 with Oak Ridge National Laboratory, managed by UT-Battelle, LLC.

Westvaco Corporation wishes to acknowledge the contributions of Dr. Ken Wilkes and Dr. Claudia Rawn (Metals and Ceramics Division, ORNL) respectively, for skillful measurements and analysis of thermal conductivity and X-ray diffraction properties of powdered activated carbon.

DISTRIBUTION

INTERNAL

1-3. T. D. Burchell, Bldg. 4508, MS 6088
4. R. A. Bradley, Bldg. 4500S, MS6161
5. K. M. Wilson, 111-B UNV, MS 6499
6. R. R. Judkins, Bldg. 4508, MS 6084
7. P. A. Carpenter, Bldg. 4500N, MS 6269
8. Office of Technical Information and Classification, 4500N, 6254

EXTERNAL

9. R. S. Kripowicz, Deputy Assistant Secretary for Fossil Energy, Department of Energy, FE-2, Forrestal Building 1000 Independence Avenue, Washington, DC 20585
10. Fred. M. Glaser, Department of Energy, Deputy Director, Office of Advanced Research, FE-72, 19901 Germantown Road, Germantown, MD 20784-1290
11. Udaya Rao, Department of Energy, Federal Energy Technology Center, 626 Cochrans Mill Road, P.O. Box 10940, MS 922-273C. Pittsburgh, PA 15236
12. Marvin I. Singer, Senior Advisor, Department of Energy, Advanced Research Policy and Planning Team, 4G-052/FORS, Washington, DC 20585
13. Robert R. Romanosky, Product Manager, Advanced Research, National Energy Technology Laboratory, 3610 Collins Ferry Road, Morgantown, WV 26507-0880

14-16. Dr. Frederick S. Baker, Westvaco, Charleston Research Center, P.O. Box 118005, Charleston, SC 29423-8005

17-19. Dr. P. Hickey, Westvaco, Charleston Research Center, P.O. Box 118005, Charleston, SC 29423-8005